

## **Infrared thermal imaging analysis in screening for toddler's fracture: A proof-of-concept study**

SAATCHI, Reza <<http://orcid.org/0000-0002-2266-0187>> and RAMLAKHAN, Shammi

Available from Sheffield Hallam University Research Archive (SHURA) at:

<https://shura.shu.ac.uk/32890/>

---

This document is the Published Version [VoR]

### **Citation:**

SAATCHI, Reza and RAMLAKHAN, Shammi (2023). Infrared thermal imaging analysis in screening for toddler's fracture: A proof-of-concept study. *Applied Sciences*, 13 (24): 13299. [Article]

---

### **Copyright and re-use policy**

See <http://shura.shu.ac.uk/information.html>

## Article

# Infrared Thermal Imaging Analysis in Screening for Toddler's Fracture: A Proof-of-Concept Study

Reza Saatchi <sup>1</sup>  and Shammi Ramlakhan <sup>2,\*</sup> 

<sup>1</sup> Department of Engineering and Mathematics, Sheffield Hallam University, Sheffield S1 1WB, UK; r.saatchi@shu.ac.uk

<sup>2</sup> Emergency Department, Sheffield Children's Hospital NHS Foundation Trust, Sheffield S10 2TH, UK

\* Correspondence: sramlakhan@nhs.net

**Abstract:** This study explored and developed high-resolution infrared thermal (HRIT) imaging for screening toddler's fractures. A toddler's fracture is a common tibial fracture in children younger than six years old. The study included 39 participants admitted to an emergency department with a suspected toddler's fracture. X-ray confirmed eight participants with a toddler's fracture (20.5%). Infrared images of participants were recorded on their index visit, focusing on region-of-interests on the injured and the contralateral (uninjured) legs. The uninjured leg acted as a thermal reference. Six statistical measures obtained from the images were analyzed. These were maximum, mean, standard deviation, median, interquartile range, and skewness. The Shapiro–Wilk test indicated that the measures were from a normal distribution. A two-sample *t*-test indicated that the majority of the six measures had significantly different means ( $p < 0.05$ ) when comparing the participants with and without a fracture. Similarly, the first principal component (PC1), obtained through principal component analysis of the six measures, was significantly different ( $p < 0.05$ ) comparing participants with and without a fracture. Visualization of the statistical measures and their PC1 demonstrated distinct clustering. This study demonstrated that HRIT imaging is valuable for screening for toddler's fractures, but a larger follow-on study will be required to confirm the findings.

**Keywords:** infrared thermal imaging; toddler's fracture; bone fracture screening; infrared thermal image processing and analysis; principal component analysis; pediatric emergency medicine; orthopedics and trauma



**Citation:** Saatchi, R.; Ramlakhan, S. Infrared Thermal Imaging Analysis in Screening for Toddler's Fracture: A Proof-of-Concept Study. *Appl. Sci.* **2023**, *13*, 13299. <https://doi.org/10.3390/app132413299>

Academic Editor: Igor Pušnik

Received: 27 November 2023

Revised: 12 December 2023

Accepted: 14 December 2023

Published: 16 December 2023



**Copyright:** © 2023 by the authors. Licensee MDPI, Basel, Switzerland. This article is an open access article distributed under the terms and conditions of the Creative Commons Attribution (CC BY) license (<https://creativecommons.org/licenses/by/4.0/>).

## 1. Introduction

A fracture results in a complete or incomplete break in the anatomic continuity of a bone. This could be due to an external force or impact such as a fall, or the effect of a medical condition such as osteoporosis, which reduces bone density. During fracture healing, fracture fixation induces direct bone formation whereas moderate stability causes endochondral ossification [1].

Bony fracture repair can be described as occurring in four phases [2]. During the initial inflammation or granulation phase, hematoma is formed in the injured bone, caused by bleeding from the site and the periosteal vessels formed within the medullary canal and beneath the periosteum [3]. During the proliferative phase, a soft callus is developed, characterized by the formation of connective tissues, including cartilage and new capillaries from pre-existing vessels [2]. During the maturing or modeling phase, a hard callus is formed, leading to woven bone, either directly from mesenchymal tissue or via an intermediate stage of cartilage. At this stage, the osteoblast-formed woven bone is mechanically weak but bridges the fracture [2]. During the final or remodeling phase, the woven bone is remodeled into stronger lamellar bone, facilitated by osteoclastic bone resorption and osteoblastic bone formation [2].

Bones are highly vascularized, receiving around 10–15% of resting cardiac output [4]. Blood supply is provided by an extensive network of arteries, arterioles, and capillaries [5].

A fracture causes inflammation and disturbs the blood flow at the injured site. The changes in the blood flow cause the temperature to change at the affected area, including the overlying skin. There is evidence of an increase in the temperature of surrounding tissues at the site of a fracture due to increases in metabolism and blood flow [6]. A temperature change can accurately be measured and analyzed by high-resolution infrared thermal imaging (HRIT).

In the following sections, studies related to applications of infrared thermal imaging to screen for bone fracture are reviewed, a brief description of the toddler's fracture is provided, the study's methodology is described, and the results are explained.

### *1.1. Infrared Imaging and Its Application in Bone Fracture Detection*

Objects with a temperature above absolute zero ( $-273.15\text{ }^{\circ}\text{C}$ ) radiate infrared (IR). IR radiation (wavelength 700 nm–1 mm) is part of the electromagnetic spectrum that can be detected using either photon detectors or thermal detectors [7]. In photon detectors, the IR radiation is absorbed by interaction with the object's electrons. An electrical signal results from a change in electronic energy distribution. These detectors exhibit excellent signal-to-noise performance and a very fast response, but they require cryogenic cooling [7]. In thermal detectors, the absorbed incident radiation increases the object's temperature, and the changes in its physical properties are used to generate an electrical output.

IR thermal imaging has received growing attention in the medical field [8,9]. A review of infrared thermal imaging for diagnosing bone fractures [10] summarized the findings of studies utilizing infrared thermal imaging for detecting fractures in the radius, ulna, carpus, metacarpal and phalanges, tibia, fibula, tarsus, metatarsal and phalanges, clavicle, scapula, and facial and spinal bones where thermal changes appear at the skin level, due to vascular physiological changes.

Infrared thermal imaging has been effective in detecting and monitoring musculoskeletal injuries [11]. Statistical analysis of infrared thermal images has demonstrated that the temperature of a fractured wrist is significantly higher than an uninjured wrist [12]. The study was based on 40 children admitted to a hospital's emergency department for an injury to one of their wrists. The participants' mean age was 10.5 years (standard deviation 2.63 years). Nineteen participants were diagnosed with a wrist fracture using X-ray radiography; the remaining 21 patients were diagnosed with a sprain. Overall, the temperature of the fractured wrists was 1.52% higher than the uninjured wrists. The temperature of sprained wrists was 0.97% higher than the uninjured contralateral wrist but, unlike the fractured wrist, the increase in temperature was not statistically significant. In a continuation of this study with the same participants, a multilayer perceptron artificial neural network was trained to differentiate between fractured and sprained wrists [13]. The method provided a sensitivity and specificity of 84.2% and 71.4%, respectively, in differentiating between wrist fractures and wrist sprains. Infrared thermal imaging has shown potential in identifying fractured thoracic vertebrae in children (number: 11; age: 5–18 years) with osteogenesis imperfecta [14]. Osteogenesis imperfecta is a genetic disorder in which bones become more fragile, thus increasing the risk of fracture. The authors concluded that infrared thermal imaging could provide a cost-effective and quick (as compared with magnetic resonance imaging or computerized tomography) modality for detecting fractures. The mean temperature of fractured distal forearms in 25 patients (mean age  $65.9 \pm 10.4$  years) were compared with the uninjured contralateral. The temperature difference initially increased up to 3 weeks and then subsided in the following weeks [6]. A related study compared the temperature difference between forearm fractures and the contralateral uninjured side in 19 children aged 4–14 years and found an increase in the temperature of the injured area followed by a reduction in the following weeks [15]. Infrared thermal imaging has been applied to detect fractures associated with leg, hand, forearm, clavicle, foot, and ankle in a study involving 45 patients [16]. The study concluded that infrared thermal imaging could be a valuable complementary diagnostic modality to the X-ray radiograph.

### 1.2. Toddler's Fracture

Pediatric tibial fractures are the second most common (after forearm fracture) type seen in young children, accounting for 15% of all fractures [17]. A toddler's fracture is a spiral tibial fracture in ambulatory infants and young children caused by a twisting injury while tripping, stumbling, or falling [18]. Its peak incidence is between ages 9 months and 3 years [19,20]. X-ray radiography is the gold standard for its diagnosis; however, the modality may not detect the fracture in a significant percentage of cases and the fracture only becomes visible on X-ray 7–10 days post-injury, when sclerosis or a periosteal reaction develops at the injured site [19]. The diagnosis is further complicated by difficulties in communicating with young children. A small study based on three cases highlighted the potential of sonography in detecting toddler's fractures [21]. The initial X-ray radiographs had not indicated a toddler's fracture, but sonography revealed a fracture hematoma by a layer of low reflectivity superficial to the tibial cortex and an elevated periosteum. A toddler's fracture, irrespective of its confirmation or presumption of occurrence, is typically treated with the immobilization of the injured leg with a cast or splint [22,23].

### 1.3. Study's Purpose and Contribution

The purpose of this study is to explore and further develop infrared thermal imaging for screening for toddler's fracture at the index presentation. The method at this stage of development aims to assist clinicians to identify children who do not have a toddler's fracture, thus avoiding the need for X-ray radiographs and revisits and unnecessarily placing the injured leg in a cast. The remaining patients would then undergo an X-ray radiograph to confirm a fracture and the standard treatment thereafter.

The contributions of this paper are:

- Devising an infrared thermal image averaging method to deal with the possible bias associated with a larger number of participants without a toddler's fracture, as compared to the participants with a toddler's fracture;
- Extraction and analysis of discriminatory measures obtained from the infrared thermal images of toddler's fracture patients, indicating a statistically significant difference between the participants with and without a toddler's fracture;
- Visualization of distinct clusters identifying the participants with a toddler's fracture;
- Principal component analysis of the statistical measures that differentiated the participants with and without a toddler's fracture;
- Demonstration that infrared thermal imaging can be valuable for screening toddler's fractures.

## 2. Materials and Methods

In this section, the methodology for participant recruitment, infrared thermal image recording, analysis, and interpretation of the information are described.

### 2.1. Recruitment

Ethical approval for the study was attained from the UK National Health Service Ethics Committee (REC Reference 20/SS/0124, IRAS project ID 280774). The study was registered on clinicaltrials.org (NCT05536622). A participant information sheet for the parents, and its simplified version for their children aged 3–5 years, were prepared. For children aged 3–5 years, the parents consented and the child assented. For children younger than 3 years, only their parents consented. The participants' personal data and their infrared thermal imaging were anonymized prior to storage and processing in accordance with the UK Data Protection Act (2018).

Participants were recruited from an urban tertiary pediatric emergency department (ED) who attended with suspicion of a toddler's fracture. The inclusion criteria were:

- Children aged up to 5 years (inclusive) admitted to the emergency department (ED) of Sheffield Children's Hospital for a leg injury suspected of a toddler's fracture;
- Triage as category D (excluding those in severe pain, or deformity);

- Children who were X-rayed as part of their routine assessment (no patient underwent an X-ray for the purpose of this study);
- Consent by parents and assent by the child (in cases of a child aged 3 years and older);
- The exclusion criteria were:
- Participants who had multiple injuries (e.g., those involved in a serious car accident);
- Participants who had difficulty understanding the nature of the study (e.g., non-native English speakers, or those with disabilities impairing their understanding of the study);
- Participants whose consent (parent) or assent (child) could not be obtained.

Altogether, 46 participants were recruited; however, in seven cases, the child was too uncooperative for recording (e.g., excessive leg movements during recording), thus their data were excluded. The analysis was based on 39 participants, eight with a toddler's fracture (confirmed by X-ray radiograph) and, for the remaining 31 cases, X-ray radiograph had not shown a fracture. Table 1 provides the details of the 39 participants included in the study.

**Table 1.** Characteristics of study participants.

Demographic Parameters	Measures
Diagnosis (confirmed by X-ray)	31 participants without a toddler's fracture 8 participants with a toddler's fracture
Participant age (years)	Mean: 1.89 Standard deviation: 1.18
Participant sex	25 males 14 females
Injury side	21 patients with injury on the right leg 18 patients with injury on the left leg
Medication	17 participants on medication (paracetamol, ibuprofen) 22 participants without medication

The details of the participants with a toddler's fracture are included in Table 2.

**Table 2.** Characteristics of participants with a toddler's fracture confirmed by X-ray radiograph.

Toddler's Fracture	Age Year (Months)	Sex	Injured Leg	Fracture Details	Fracture Confirmation	Medication
1	2 (2)	Male	Right	Trampoline fracture, non-displaced transverse right proximal tibial fracture	Second visit	Nil
2	2	Female	Left	Un-displaced transverse fracture tibial metaphysis	First visit	Paracetamol
3	2 (2)	Male	Left	Spiral fracture of the tibia, buckle fracture of the proximal fibula	First visit	Ibuprofen
4	1 (10)	Female	Right	Distal toddler's fracture	First visit	Nil
5	0 (11)	Female	Left	Mid-proximal toddler's fracture	Second visit	Paracetamol
6	1 (7)	Male	Right	Proximal, buckle fracture	First visit	Paracetamol and Ibuprofen
7	2 (6)	Female	Right	Proximal, buckle fracture	First visit	Paracetamol
8	1 (0)	Female	Right	Distal, minor buckle	First visit	Nil

## 2.2. Data Acquisition

Prior to infrared thermal imaging, the participant's relevant details were recorded. These included:

- Age;
- Sex;
- Time and date of the injury;
- Time and date of arrival at the hospital;
- Details of any medication taken;
- Cause of the injury;
- Diagnosis type (fracture or not fracture) using an X-ray radiograph on an initial admission and, if required, the follow-on visit to the hospital;
- Fracture details in cases where fracture is confirmed.

A dedicated room close to the X-ray imaging department was used for infrared thermal imaging. The room did not have heat sources that could have interfered with the recording. The single window in the room was kept closed and the recording was kept furthest from the window. Any possible sources of draught were minimized. Temperature variations in the recording room conformed to be within the acceptable range of 18–25 °C [24].

To the best of our knowledge, there has not been a study determining the minimum requirements (e.g., temperature sensitivity, image resolution, etc.) for the infrared thermal camera to screen bone fractures; however, the camera needs to be able to differentiate between temperature changes caused by the injury, resulting in a fracture, and those without a fracture. Cameras with higher specifications tend to be significantly more expensive; therefore, there is a balance between cost vs. a camera's ability to carry out the expected task. The infrared thermal camera used in this study was a FLIR T630sc (Teledyne FLIR, Wilsonville, OR, USA) [25]. The camera's noise-equivalent temperature difference (NETD: a measure indicating how well the camera can differentiate between very small differences in infrared thermal radiation) is less than 40 mK; its image resolution is 640 × 480 pixels; its spectral range is 7.5 μm–13 μm; its dynamic range is 14 bits; its operating temperature is −14 °C–50 °C; and the camera's integrated lens is 18 mm (25°). A computer, connected to the camera, facilitated data storage. Emissivity was set to 0.95, which is suitable for human body infrared thermal recordings. The participants acclimatized to the recording room temperature for 10 min prior to the recordings. The 10-min acclimatization period struck a balance between ensuring the participants (very young children) were accustomed to the room temperature and ensuring their cooperation with the recording. The aim was to minimize their hospital stay at a time when they might be stressed due to their injury while obtaining suitable recordings. This period was in line with our study's ethical approval. The infrared thermal camera was kept in the recording room, thus it did not need acclimatization. The distance between the camera and the participant was 1 m.

For the recording, the participant sat on the side of hospital bed with their legs uncovered and clearly visible in the thermal camera's field of view. In some cases, parents held their child by sitting next to them for safety and reassurance. The data analysis was carried out using Matlab® (version R2023b, Mathworks Inc., Cambridge, UK [26]).

A 10-s video (frame rate 30 frames per second) was recorded. This allowed for the averaging of the recorded frames (across the 300 frames) to reduce thermal noise.

## 2.3. Data Processing

To analyze the recorded infrared thermal images for each participant, the following tasks were performed using Matlab®:

- The recorded video of a participant was loaded into Matlab®;
- The first image of the video was displayed on the computer screen;
- Using the cropping function (of Matlab®), a region of interest (ROI) of the injured leg, covering from just above the ankle to just below the knee, was manually cropped from

the first image. The contour of the region followed the edge of the leg. This formed the template;

- The template was then used to automatically select the same region from the remaining 299 images of the video. As there could have been small leg movements during the recording, a template-matching tracking algorithm was used to ensure the selected sections aligned. This algorithm selected a section that provided the highest correlation with the template [27,28];
- The template was then averaged with the selected ROI sections on the following images;
- The above steps were repeated for the contralateral (not injured) leg;

The above operations resulted in two images representing the ROI for the injured leg and its contralateral (uninjured) leg.

#### 2.4. Statistical Features of the Region of Interest

As it was not clear which statistical measures best characterized the ROI, six measures were extracted from the selected ROI (for both the injured and contralateral uninjured legs). These were (i) maximum, (ii) mean, (iii) standard deviation, (iv) median, and (v) interquartile range (IQR) characterizing temperature magnitude. The distribution of ROI temperature was represented by (v) skewness. Skewness is a measure of the asymmetry of probability distribution about its mean value.

The measures from the uninjured contralateral leg were subtracted from those from the injured leg. The contralateral leg acted as temperature reference (control) as skin temperature in healthy subjects can vary and, thus, by this subtraction, this effect was reduced.

The number of participants without a fracture was much larger than participants with a fracture (i.e., eight with a fracture against 31 without a fracture). This imbalance might have biased the follow-on statistical analysis toward non-fracture cases. To reduce this imbalance, an averaging operation illustrated in Figure 1 was devised and was applied to the participants without a fracture. The procedure selected the participant (without a fracture) from the top of the list, used the Euclidean distance to identify a participant from the list whose feature set was closest to the selected participant, averaged their two feature sets (i.e., the six statistical measures), retained the averaged feature set, and excluded both participants whose feature sets were averaged from the list. Following each averaging, a new participant, not yet excluded, moved to the top of the list, and the operation was repeated until all participants had been processed.

A single application of the method reduced the number of participants without a fracture from 31 to 15. It was possible to further reduce the number of participants without a fracture by applying the method for the second round, starting with the averaged feature sets obtained from the previous round; however, further reduction was not undertaken given that the difference between participants with and without a fracture had already been reduced to 7.

Statistical tests of significance (outlined in the next section) and principal component analysis (PCA) of the six statistical measures were carried out to differentiate between the participants with and without a fracture.

#### 2.5. Statistical Tests of Significance

The Shapiro–Wilk test was used to determine whether the six statistical measures were from a normal distribution. For this test, the null hypothesis is that the population is from a normal distribution. The hypothesis is rejected when statistical probability ( $p$ -value) is less than 0.05 for 95% confidence interval.

To determine whether there was a statistically significant difference between the six statistical measures when comparing the participants with and without a fracture, the two-sample  $t$ -test and two-sided Wilcoxon rank sum test [29] were considered. The two-sample  $t$ -test performs a test of the hypothesis ( $H$ ) that two independent samples (that can have different lengths) are from distributions with equal means. It performs an unpaired two-

sample *t*-test. The data are assumed to be from normal distributions with unknown, but equal, variances. It returns a probability value (*p*) that, when less than 0.05 (corresponding to  $H = 1$ ), indicates that the null hypothesis (i.e., equal mean values) can be rejected at the 5% significance level. The two-sided Wilcoxon rank sum test is a non-parametric test used to establish whether two groups' medians are equal. Its hypothesis is that they have an equal median. It is equivalent to a Mann–Whitney U-test and assumes the two groups are independent. At 5% significance level, probability values less than 0.05 result in the rejection of the null hypothesis of equal medians.

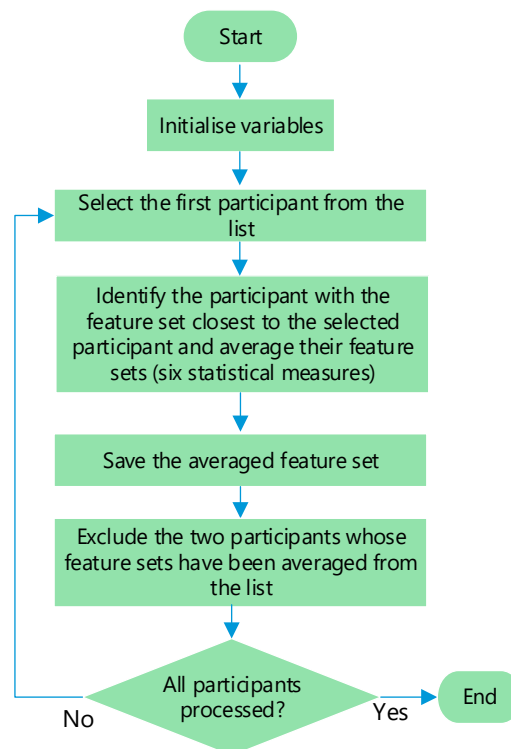


**Figure 1.** The averaging operation for non-fracture participants.

### 3. Results

A typical infrared thermal image of a participant with a toddler's fracture is shown in an RGB format in Figure 2a. The participant was a 14-month male with a toddler's fracture of his right leg. The fracture was not detected by X-ray radiography on the first attendance to the hospital. The injured leg was put into a cast and the participant underwent another X-ray on the second visit, 10 days later. It was then confirmed as a toddler's fracture (non-displaced transvers right proximal tibial fracture). The infrared thermal image of the right leg was relatively warmer (brighter colour) as compared with the uninjured left leg. Although visual inspection of an infrared image (Figure 2a) may highlight temperature anomalies associated with an injury, image and data analysis are still required for a conclusive interpretation [12,13]. The image process was carried out on the temperature image (matrix of temperature values) shown in Figure 2b (not on RGB images).

Figure 3a,b show infrared thermal images for a male participant, aged 3 years and 9 months, admitted with an injury to the right leg, in an RGB format and as a temperature format, respectively. The participant had an X-ray radiograph on the first hospital visit, but a fracture could not be confirmed. The injured leg was put in a cast and X-rayed again two weeks later, when the absence of a fracture was confirmed.

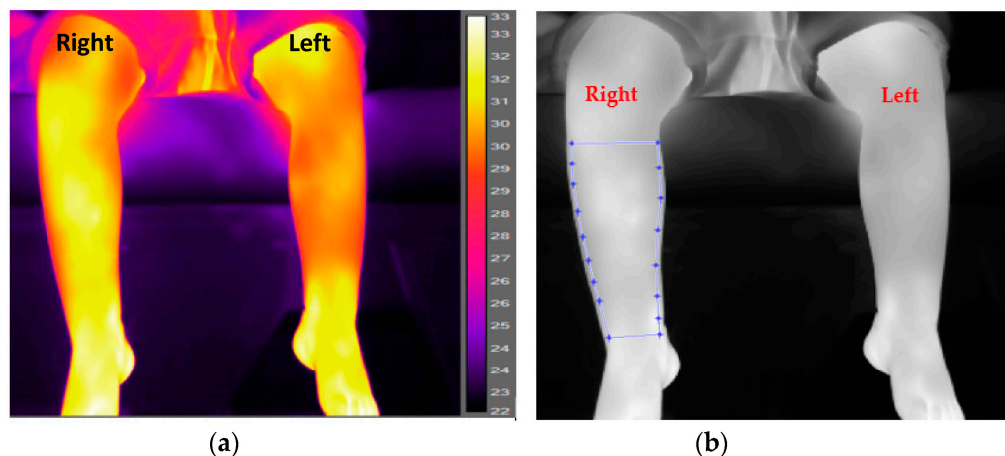


**Figure 2.** An example of an infrared thermal image for a participant diagnosed by X-ray to have a toddler's fracture of the right tibia. (a) RGB format; (b) processed temperature image indicating the cropped region of interest on the right leg (the uninjured left leg was similarly cropped).

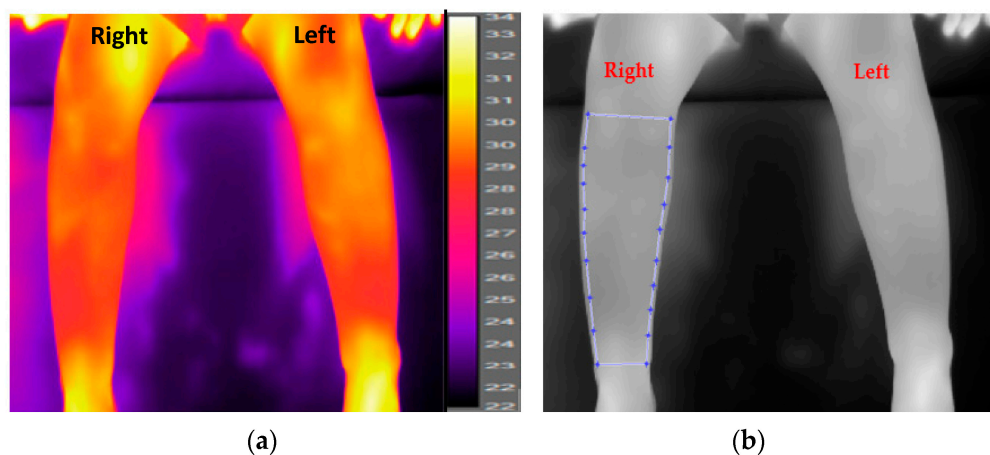
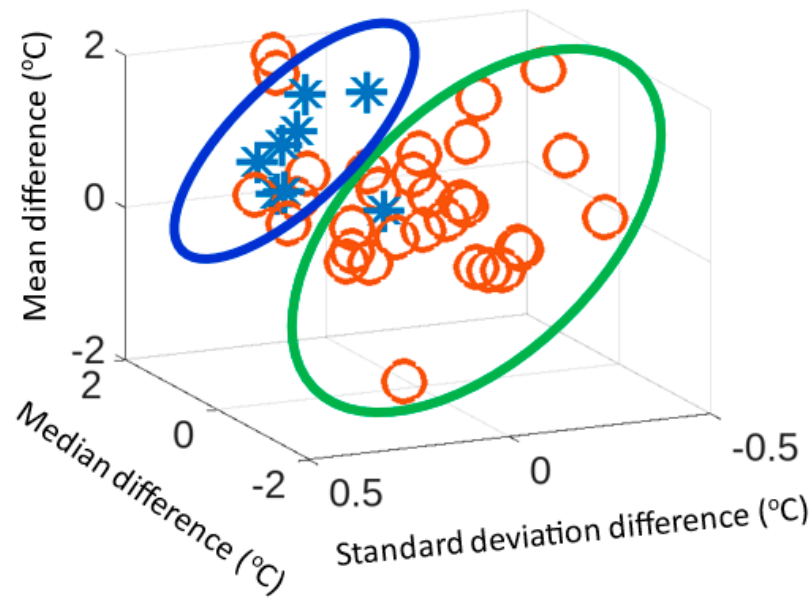


**Figure 3.** Infrared thermal image (a) RGB format, (b) temperature image of a participant diagnosed by an X-ray as not having a toddler's fracture (right leg injury). The temperature image indicates the cropping of the ROI on the right leg. The uninjured left leg was similarly cropped.

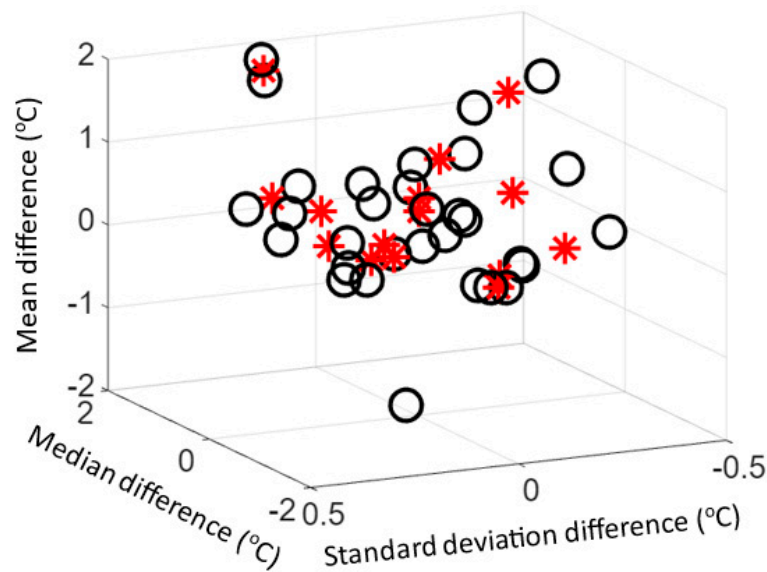
As an illustration, a scatter plot of median, standard deviation, and mean temperature difference (i.e., the temperature difference between the injured and uninjured legs) is provided in Figure 4. The plot includes all eight participants with a fracture (shown as asterisks) and 31 participants without a fracture (shown as circles). Two distinct clusters were identifiable, representing fracture and not fracture groupings. Although most participants were correctly clustered, there were a few participants appearing in the wrong clusters.

Figure 5 shows a scatter plot of median, standard deviation, and mean temperature difference illustrating the application of the averaging method (outlined in Figure 1) to the 31 participants without a fracture (represented by black circles) to reduce their number to 15 (shown by red asterisks).

Table 3 shows the temperature difference between the injured and uninjured (contralateral) legs for the eight participants with a fracture and 15 averaged participants without a fracture. The maximum temperature measure showed a 60.2% difference between the injured legs resulting in a fracture and not fracture. Similarly, the mean temperature measure shows a 59.6% difference between the injured legs resulting in a fracture and not fracture.



**Figure 4.** A scatter plot of median, standard deviation, and mean temperature difference between fractured (represented by asterisks) and uninjured legs (represented by circles).



**Figure 5.** A scatter plot of median, standard deviation, and mean temperature difference illustrating the application of the averaging method (outlined in Figure 1) to the 31 participants without a fracture (represented by black circles) to reduce the number to 15 (represented by red asterisks).

**Table 3.** Averaged statistical measures indicating differences between the participants with a toddler’s fracture ( $n = 8$ ) and participants without a toddler’s fracture ( $n = 15$ ).

Statistical Measure	Mean		Standard Deviation	
	Fracture	Not Fracture	Fracture	Not Fracture
Maximum (°C)	1.097	0.437	0.676	0.993
Mean (°C)	0.882	0.356	0.442	0.582
Standard deviation	0.177	−0.036	0.116	0.203
Median (°C)	0.891	0.365	0.397	0.609
Skewness	−0.346	0.030	0.786	0.560
Interquartile range (°C)	0.193	−0.091	0.196	0.324

Principal component analysis of the six statistical features (shown in Table 3) was used to explore the extent to which it could characterize the participants with and without a fracture. A scree plot (shown in Figure 6) was used to determine the number of principal components to retain. This is a plot of eigenvalues of the six statistical measures against their principal component number. Typically, the “elbow” of the plot, where the eigenvalues seem to level off, is considered, and the principal components to its left are retained as the most significant. The plot’s elbow was between the 3rd and 4th principal component number and, thus, the first three principal components were selected. The eigenvalues represent the total amount of variance explained by each associated principal component. The main three principal components accounted for 97.0% of the overall variance.

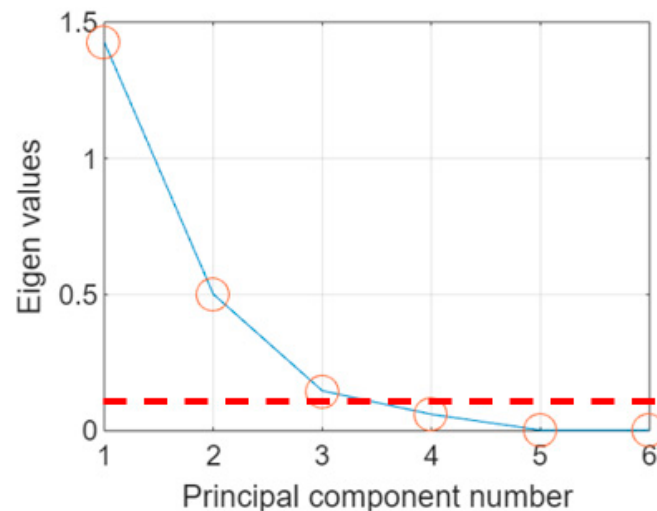


**Figure 6.** The scree plot of the six statistical measures.

The plot of three main principal components is shown in Figure 7. Two distinct clusters representing participants with a fracture (represented asterisks) and participants without a fracture (represented by circles) were identifiable. The majority of the participants were clustered according to their injury types (fracture or not fracture).

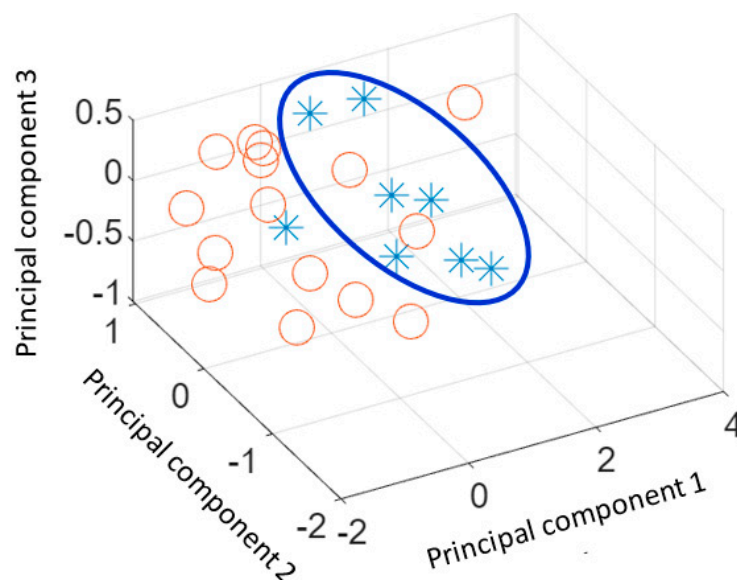


**Figure 7.** Plot of the three main principal components. The circles represent participants without a fracture and asterisks represent participants with a fracture.

The application of the Shapiro–Wilk test indicated that all six statistical measures were from a normal distribution (i.e.,  $p > 0.05$ ); therefore, a  $t$ -test was used to establish whether the means associated with the fracture and not fracture statistical measures were significantly different (given the statistical measures were from a normal distribution, the Wilcoxon rank sum test was not required). The results are provided in Table 4. They indicated that mean, standard deviation, median, and interquartile range had probabilities (significance level 5%) less than 0.05 and, thus, a significant difference between their means when comparing the two injury types (fracture and not fracture) was registered.

**Table 4.** Shapiro–Wilk and two-sample  $t$ -test results for the six statistical measures.

Statistical Measure	Probability ( $p$ )	
	Shapiro–Wilk Test	$t$ -Test
Maximum	0.235	0.1084
<b>Mean</b>	<b>0.579</b>	<b>0.0370</b>
<b>Standard deviation</b>	<b>0.136</b>	<b>0.0129</b>
<b>Median</b>	<b>0.898</b>	<b>0.0394</b>
Skewness	0.613	0.1962
<b>Interquartile range</b>	<b>0.223</b>	<b>0.0350</b>

As an illustration, a scatter plot of median, standard deviation, and mean temperature difference between injured and uninjured legs is provided in Figure 8. Red asterisks represent the eight participants with a fracture and black circles represent the 15 participants (averaged) without a fracture. Seven participants with a fracture were observed in a cluster, although a participant with fracture and one participant without a fracture were not represented correctly.

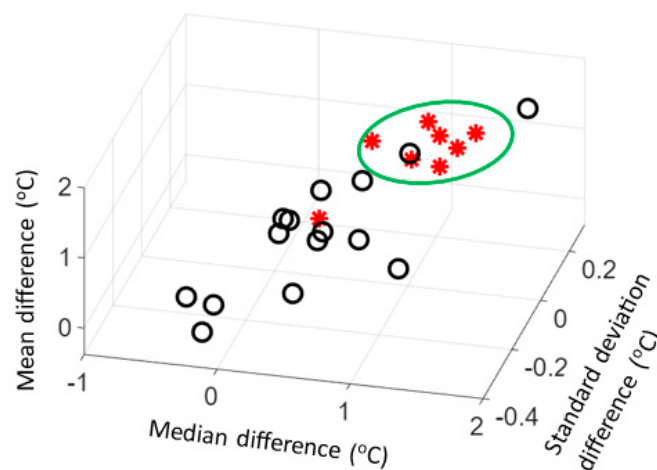


**Figure 8.** Scatter plot of median, standard deviation, and mean temperature difference between injured and uninjured legs. Red asterisks represent the eight participants with a fracture and black circles represent 15 participants without a fracture.

Table 5 provides the mean and standard deviation values for the main three principal components for participants with and without a fracture.

**Table 5.** Mean and standard deviation values for the main three principal components for participants with and without a fracture.

Principal Component (PC)	Mean		Standard Deviation	
	Fracture	Not Fracture	Fracture	Not Fracture
PC1	0.665	−0.355	0.797	1.240
PC2	−0.263	0.140	0.835	0.615
PC3	0.130	−0.070	0.275	0.421

Table 6 provides the statistical tests results for the three main principal components. The Shapiro–Wilk tests indicated all three principal components were from a normal distribution ( $p > 0.05$ ). The application of the  $t$ -test indicated that the difference between the mean of the first principal component for the participants with and without a fracture was statistically significant ( $p < 0.05$ ).

**Table 6.** Statistical tests for the three main principal components.

Principal Component (PC)	Probability	
	Shapiro-Wilk Test	$t$ -Test
PC1	<b>0.417</b>	<b>0.0485</b>
PC2	0.424	0.2005
PC3	0.122	0.2420

#### 4. Discussion

This study indicated that infrared thermal imaging has potential for screening for toddler’s fractures on the index ED visit; however, suitable data processing and analysis are required to ensure that the images are suitably analysed and interpreted. Its finding is in line with earlier work that utilised infrared thermal imaging to screen or detect bone fractures [6,10,12–15,30]. Infrared thermal imaging can be performed quickly, without the need for extensive training. It is harmless, non-contact, and highly cost effective. If the diagnosis of a toddler’s fracture cannot be confirmed following an X-ray radiograph, the injured leg is placed in a cast and the leg is X-rayed again after about 10 days. In cases where the leg is not fractured, the child is unnecessarily inconvenienced by the cast and by exposure to X-ray radiation. There is also the cost implication of unnecessary casting, revisits, and repeat X-rays.

This was a proof-of-concept study, given the number of participants included; therefore, a larger study will be required to provide greater confidence in infrared thermal imaging as a routine clinical tool in ED environments. The temperature of the injured area changes with time, initially increasing, reaching a peak, and then gradually decreasing. The time since injury (i.e., the time between the occurrence of the injury and the patient attending the hospital) varied for the participants. As this measure was not included in the analysis, it may have negatively affected the results and, thus, requires further exploration; however, all children were imaged within 72 h of the injury. Similarly, some participants had taken medication (analgesics with antipyretic properties) and, thus, the possible effect of the medication on the results needs to be considered.

An important issue is the severity of the injury, either resulting in a fracture or not fracture. This was not considered in this study but may have negatively affected the results. This study used a 10-s video recording; however, in future work, an exploration will be carried out to establish whether a single image could be sufficient.

The scatter plots of Figures 4, 7 and 8 indicated that a few participants were not grouped correctly in accordance with their injury diagnosis. Further investigation of image processing and feature extraction techniques may help to improve the differentiation.

In this study, given the number of participants, a pattern recognition approach was not used to differentiate between participants with and without a fracture. In follow-on studies,

this would be considered. Artificial intelligence methods relevant to ED practice [31–33] will also be explored in more detail.

This study included infrared thermal images taken from the front of the leg. During the follow-on study, infrared thermal images recorded from the sides of the legs will be combined with the image recorded from the front of the leg to explore further improvement of the results.

This study's findings were promising and justify the need for a larger study. It applied a variety of statistical and imaging techniques, including principal component analysis and infrared thermal images, to illustrate an innovative approach to screening for toddler's fractures.

## 5. Conclusions

Bone fractures are one of the main causes of attendance to emergency departments (EDs). Tools that can improve the utilization of ED resources and enhance patient experience are valuable. In the case of a toddler's fracture, given that, in many cases, the fracture may not be detected during the first ED visit, there is a clear need for improvement in screening and diagnosis.

Statistical measures representing the features of the infrared images of participants with and without a toddler's fracture indicated a significant temperature difference between the two injury types. This study's finding, highlighting the potential of infrared imaging in screening for bone fractures, is in line with earlier work. The main contribution of this study was the demonstration of significant differences in statistical features extracted from participants with and without a toddler's fracture. As the participants without a fracture were much larger than those with a fracture, an averaging method was devised to reduce the imbalance and minimise possible bias toward the not fracture group.

Infrared thermal imaging is a cost-effective, harmless, and easily applicable technology that is receiving growing interest in medical diagnosis and monitoring. Its application to screening or diagnosing bone fractures is an emerging technology.

**Author Contributions:** Conceptualization, R.S. and S.R.; methodology, R.S. and S.R.; software, R.S.; validation, R.S. and S.R.; formal analysis, R.S. and S.R.; investigation, R.S. and S.R.; resources, R.S. and S.R.; data curation, R.S. and S.R.; writing—original draft preparation, R.S. and S.R.; writing—review and editing, R.S. and S.R.; visualization, R.S. and S.R.; project administration, R.S. and S.R. All authors have read and agreed to the published version of the manuscript.

**Funding:** This research received research funding from the Research England Grow MedTech (<https://growmed.tech/>) consortium. The Sheffield Children's Hospital Charity (<https://www.tchc.org.uk/>) funded the infrared camera used in the study.

**Institutional Review Board Statement:** The study was conducted in accordance with the Declaration of Helsinki and approved by the U.K. National Health Service Ethics Committee (REC Reference 20/SS/0124, IRAS project ID 280774).

**Informed Consent Statement:** Informed consent was obtained from all subjects involved in the study. None of the participants can be identified in this article.

**Data Availability Statement:** The data presented in this study are available on request from the corresponding author. Patient data are not shared due to ethical restrictions.

**Acknowledgments:** The authors are grateful to all participants (patients and their carers) who kindly took part.

**Conflicts of Interest:** The authors declare no conflict of interest.

## References

1. Claes, L.; Recknagel, S.; Ignatius, A. Fracture healing under healthy and inflammatory conditions. *Nat. Rev. Rheumatol.* **2012**, *8*, 133–143. [[CrossRef](#)] [[PubMed](#)]
2. Marsh, D.R.; Li, G. The biology of fracture healing: Optimising outcome. *Br. Med. Bull.* **1999**, *55*, 856–869. [[CrossRef](#)] [[PubMed](#)]

3. Oryan, A.; Monazzah, S.; Bigham-Sadegh, A. Bone injury and fracture healing biology. *Biomed. Environ. Sci.* **2015**, *28*, 57–71. [PubMed]
4. Watson, E.C.; Adams, R.H. Biology of bone: The vasculature of the skeletal system. *Cold Spring Harb. Perspect. Med.* **2018**, *8*, a031559. [CrossRef] [PubMed]
5. Draghici, A.; Taylor, J.A. Mechanisms of bone blood flow regulation in humans. *Appl. J. Physiol.* **2021**, *130*, 772–780. [CrossRef] [PubMed]
6. Halužan, D.; Davila, S.; Antabak, A.; Dobric, I.; Stipic, I.; Augustin, G.; Ehrenfreund, T.; Prlić, I. Thermal changes during healing of distal radius fractures—Preliminary findings. *Injury* **2015**, *46*, S103–S106. [CrossRef] [PubMed]
7. Rogalski, A. Infrared detectors: An overview. *Infrared Phys. Technol.* **2002**, *43*, 187–210.
8. Sousa, E.; Vardasca, R.; Teixeira, S.; Seixas, A.; Mendes, J.; Costa-Ferreira, A. A review on the application of medical infrared thermal imaging in hands. *Infrared Phys. Technol.* **2017**, *85*, 315–323. [CrossRef]
9. Owen, R.; Ramlakhan, S. Infrared thermography in paediatrics: A narrative review of clinical use. *BMJ Paediatr. Open* **2017**, *1*, e000080. [CrossRef]
10. Strasse, W.A.D.; Ranciaro, M.; De Oliveira, K.R.G.; Campos, D.P.; Mendonça, C.J.A.; Soni, J.F.; Mendes, J.; Nogueira-Neto, N.; Nohama, P. Thermography applied in the diagnostic assessment of bone fractures. *Res. Biomed. Eng.* **2022**, *38*, 733–745. [CrossRef]
11. Sanchis-Sánchez, E.; Vergara-Hernández, C.; Cibrián, R.M.; Salvador, R.; Sanchis, E.; Codoñer-Franch, P. Infrared thermal imaging in the diagnosis of musculoskeletal injuries: A systematic review and meta-analysis. *Am. J. Roentgenol. AJR* **2014**, *203*, 875–882. [CrossRef] [PubMed]
12. Reed, C.; Saatchi, R.; Burke, D.; Ramlakhan, S. Infrared thermal imaging as a screening tool for paediatric wrist fractures. *Med. Biol. Eng. Comput.* **2020**, *58*, 1549–1563. [CrossRef] [PubMed]
13. Shobayo, O.; Saatchi, R.; Ramlakhan, S. Infrared thermal imaging and artificial neural networks to screen for wrist fractures in pediatrics. *Technologies* **2022**, *10*, 119. [CrossRef]
14. De Salis, A.F.; Saatchi, R.; Dimitri, P. Evaluation of high resolution thermal imaging to determine the effect of vertebral fractures on associated skin surface temperature in children with osteogenesis imperfecta. *Med. Biol. Eng. Comput.* **2018**, *56*, 1633–1643. [CrossRef]
15. Ćurković, S.; Antabak, A.; Halužan, D.; Luetić, T.; Prlić, I.; Šiško, J. Medical thermography (digital infrared thermal imaging—DITI) in paediatric forearm fractures—A pilot study. *Inj. Int. J. Care Inj.* **2015**, *46S*, S36–S39. [CrossRef]
16. Strasse, W.A.D.; Campos, D.P.; Mendonça, C.J.A.; Soni, J.F.; Mendes, J.; Nohama, P. Detecting bone lesions in the emergency room with medical infrared thermography. *BioMed. Eng. OnLine* **2022**, *21*, 35. [CrossRef]
17. Weber, B.; Kalbitz, M.; Baur, M.; Braun, C.K.; Zwingmann, J.; Pressmar, J. Lower leg fractures in children and adolescents—Comparison of conservative vs. ECMES treatment. *Front. Pediatr. Sect. Pediatr. Orthop.* **2021**, *9*, 597870. [CrossRef]
18. Alqarni, N.; Goldman, R.D. Management of toddler’s fractures. *Can. Fam. Physician Méd. Fam. Can.* **2018**, *64*, 740–741.
19. Pelayoa, S.L.; Fernández, J.R.; Cabelloa, M.T.L.; Lorenzoc, M.R.; Alfaroc, M.D.G.; Jiménez, C.A. Current diagnosis and management of toddler’s fracture—Manejo diagnóstico y terapéutico actual de la fractura de los primeros pasos. *An. Pediatr.* **2020**, *92*, 262–267. [CrossRef]
20. Seyahi, A.; Uludag, S.; Altıntaş, B.; Demirhan, M. Tibial torus and toddler’s fractures misdiagnosed as transient synovitis: A case series. *J. Med. Case Rep.* **2011**, *5*, 305. [CrossRef]
21. Lewis, D.; Logan, P. Sonographic diagnosis of toddler’s fracture in the emergency department. *J. Clin. Ultrasound* **2006**, *34*, 190–194. [CrossRef] [PubMed]
22. Townley, S.; Messahel, S.; Korownyk, C.; Morely, E.; Perry, D.C. Is immobilisation required for toddler’s fracture of the tibia? *BMJ* **2022**, *379*, e071764. [CrossRef] [PubMed]
23. Schuh, A.M.; Whitlock, K.B.; Klein, E.J. Management of toddler’s fractures in the pediatric emergency department. *Pediatr. Emerg. Care* **2016**, *32*, 452–454. [CrossRef] [PubMed]
24. Ammer, K.; Ring, F.J. *Medical Infrared Imaging: Principles and Practice*; Diakides, M., Bronzino, J.D., Perterson, D.R., Eds.; CRC Press, Taylor and Francis Group: Boca Raton, FL, USA, 2012.
25. FLIR. Available online: <https://www.flir.co.uk/> (accessed on 20 October 2022).
26. MathWorks©. Available online: <https://uk.mathworks.com/> (accessed on 17 November 2023).
27. Lewis, J.P. Fast template matching. In Proceedings of the Vision Interface 95, Canadian Image Processing and Pattern Recognition Society, Quebec City, QC, Canada, 15–19 May 1995; pp. 120–123. Available online: [http://scribblethink.org/Work/nvisionInterface/vi95\\_lewis.pdf](http://scribblethink.org/Work/nvisionInterface/vi95_lewis.pdf) (accessed on 24 October 2019).
28. Brunelli, R. *Template Matching Techniques in Computer Vision: Theory and Practice*; Wiley: Hoboken, NJ, USA, 2009; ISBN 978-0-470-51706-2.
29. Mann, P.S.; Lacke, C.J. *Introduction to Statistics*; John Wiley & Sons, Inc.: Hoboken, NJ, USA, 2001.
30. Owen, R.; Ramlakhan, S.; Saatchi, R.; Burke, D. Development of a high-resolution infrared thermographic imaging method as a diagnostic tool for acute undifferentiated limp in young children. *Med. Biol. Eng. Comput.* **2018**, *56*, 1115–1125. [CrossRef]
31. Bora, E.S. Artificial intelligence in medicine. *J. Exp. Basic Med. Sci.* **2023**, *4*, 33–36.

32. Chenais, G.; Lagarde, E.; Gil-Jardiné, C. Artificial intelligence in emergency medicine: Viewpoint of current applications and foreseeable opportunities and challenges. *J. Med. Internet Res.* **2023**, *25*, e40031. [[CrossRef](#)]
33. Jalal, S.; Parker, W.; Ferguson, D.; Nicolaou, S. Exploring the role of artificial intelligence in an emergency and trauma radiology department. *Can. Assoc. Radiol. J.* **2021**, *72*, 167–174. [[CrossRef](#)]

**Disclaimer/Publisher’s Note:** The statements, opinions and data contained in all publications are solely those of the individual author(s) and contributor(s) and not of MDPI and/or the editor(s). MDPI and/or the editor(s) disclaim responsibility for any injury to people or property resulting from any ideas, methods, instructions or products referred to in the content.